Photoacoustic technique for the characterization of plasmonic properties of 2D periodic arrays of gold nanoholes

E. Petronijevic, G. Leahu, V. Mussi, C. Sibilia, and F. A. Bovino

Citation: AIP Advances **7**, 025210 (2017); doi: 10.1063/1.4977545
View online: http://dx.doi.org/10.1063/1.4977545
View Table of Contents: http://aip.scitation.org/toc/adv/7/2
Published by the American Institute of Physics

Photoacoustic technique for the characterization of plasmonic properties of 2D periodic arrays of gold nanoholes

E. Petronijevic,[1,a] G. Leahu,[1] V. Mussi,[2] C. Sibilia,[1] and F. A. Bovino[1,3]
[1]*Department S.B.A.I., La Sapienza, Rome, I-00161, Italy*
[2]*Institute for Complex Systems ISC-CNR, National Research Council, 00133 Rome, Italy*
[3]*Quantum Technologies Lab, Leonardo-Finmeccanica, Via Tiburtina, Km.12.400, Rome, Italy*

(Received 1 July 2016; accepted 12 February 2017; published online 24 February 2017)

We apply photo-acoustic (PA) technique to examine plasmonic properties of 2D periodic arrays of nanoholes etched in gold/chromium layer upon a glass substrate. The pitch of these arrays lies in the near IR, and this, under appropriate wave vector matching conditions in the visible region, allows for the excitation of surface plasmon polaritons (SPP) guided along a dielectric – metal surface. SPP offered new approaches in light guiding and local field intensity enhancement, but their detection is often difficult due to the problematic discrimination of their contribution from the overall scattering. Here PA measures the energy absorbed due to the non-radiative decay of SPPs. We report on the absorption enhancement by presenting the spatial mapping of absorption under the incidence angles and wavelength that correspond to the efficient excitation of SPPs. Moreover, a comparison with optical transmission measurements is carried out, underlining the applicability and sensitivity of PA technique. [http://dx.doi.org/10.1063/1.4977545]

Plasmonic arrays of nanoholes have been widely investigated due to the possibility of exciting surface plasmon polaritons (SPP) – surface electromagnetic waves existing at the metal-insulator interfaces, that can be taught of as a combination of coupled light and surface waves of conducting electrons in the metal.[1] SPP can be excited under a phase-matching condition which can be provided e.g. by the coupling of the incoming field with the Bloch waves of the periodical structure. Accordingly, the formed coherent superposition of propagating SPP is called Bloch-wave SPP (BWSPP), and its resonant wavelengths can be found from the phase matching condition for the case of 2D grating under oblique incidence:[2]

$$\frac{2\pi}{\lambda}\sqrt{\frac{\varepsilon_m(\lambda)\,\varepsilon_d(\lambda)}{\varepsilon_m(\lambda)+\varepsilon_d(\lambda)}} = \frac{2\pi n}{\lambda} sin\Theta(u_x+u_y) \pm n_x\frac{2\pi}{p}(u_x) \pm n_y\frac{2\pi}{p}(u_y), \tag{1}$$

where $\varepsilon_m(\lambda)$ and $\varepsilon_d(\lambda)$ are the permittivity of metal and dielectric, respectively, n is the refractive index of the medium of the incident light, p is the periodicity of the array, n_x and n_y are the Bloch orders of the grating in x and y directions, and Θ is the angle of incidence. Here u_x and u_y are the unit reciprocal vectors of the periodic lattice in x and y directions; they encompass the azimuthal rotation of the sample with respect to the alignment with order (1,0): $u_x = n_x cos(\varphi) + n_y cos(\varphi + \pi/2)$, $u_y = n_x sin(\varphi) + n_y sin(\varphi + \pi/2)$. In the following we will use notation SPP (n_x, n_y) for Au-air BWSPP of orders n_x and n_y in x and y direction, respectively. The real part of the solution of Eq. (1) represents the resonant wavelengths at which SPPs are excited. The negative imaginary part of Eq. (1), converted to frequency, gives the nonradiative damping of SPP due to their coupling with metal absorption losses. The overall transmission is consequently governed by two interfering processes:[3] a resonant contribution due to the existence of discrete SPP

[a]emilija.petronijevic@uniroma1.it

resonances, and a non-resonant continuous contribution, i.e. direct scattering of the field through the 2D grating,[4,5] e.g. structure with 2D periodic subwavelength holes.[6–8] If the incidence angle and material properties are known, the solutions of Eq. (1) give the wavelengths where the resonance will take place thus affecting transmission, reflection and absorption. Excitation of these surface waves gives rise to interesting phenomena such as extraordinary optical transmission[9] and very strong localization of electrical field[10] that can be further controlled and used in subwavelength microscopy,[11] surface enhanced Raman spectroscopy (SERS),[12] plasmonic waveguides,[13] nonlinear photonics,[14] photonic integrated circuits[15] etc. For these reasons, it is important to have a low-cost, simple and reliable technique in order to be able to characterize with high sensitivity samples where SPP can be excited and manipulated.

In this work we examine the plasmonic properties of 2D nanopatterned periodic holes etched in Au and Cr (50 nm and 5 nm thick, respectively) layers upon a glass substrate. We have analyzed two different kinds of samples with different pitch, named in the following as *small* and *big* samples. The plasmonic structures have been produced by means of focused ion beam milling. The *small* samples have the periodicity of holes from $p = 744$ nm to $p = 770$ nm and the diameter $D \approx 250$nm, while the *big* ones have periodicity from $p = 1280$ nm to $p = 1470$ nm and $D \approx 390$ nm. The nanoholes were etched inside square areas of dimensions $(12.5 \times 12.5)\ \mu m^2$ and $(37 \times 37)\ \mu m^2$, around which there are scattering rings of radiuses 24 μm and 50 μm, for the *small* and the *big* samples, respectively. The scattering rings in such samples serve to scatter SPP, excited in the periodic structure and then guided along the interface, in order to see them through the transmission spectra. In Fig. 1 the AFM images show the geometrical features for the two particular samples that we have focused on. We had previously done spectral characterization[16] that shows pronounced SPP (0,1) and SPP (1,1) Fano-like resonances in the far-field transmission, shifted around 4% with respect to those obtained from Eq. (1). These red shifts, commonly found in literature and ascribed to an additional radiation damping,[11] are taken into account during the interpretation of our following results. These linear transmission measurements compared with finite-difference time-domain simulations also confirmed our hypothesis that the Au layer is completely etched, so that there is no gold at the bottom of the holes.

The photo-acoustic (PA) technique is a type of photothermal techniques, where absorption of incoming light beam leads to a non-radiative de-excitation process which generates heat, thus changing the thermal state of the sample.[17,18] If the intensity of the light is modulated in time, a sample in an air-tight chamber heats up and cools down in a cycle and, not having time to expand and contract, corresponding changes in pressure arise. These pressure changes produce an acoustic signal which is then directly converted into an electrical one by a sensitive microphone. The microphone receives the signal from the sample through the small diameter tunnel (labyrinth) so that the light cannot impinge

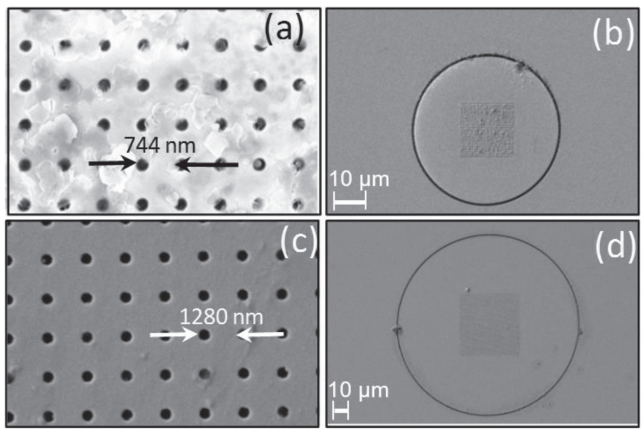

FIG. 1. AFM images of the samples. (a), (b) The small sample with p=744 nm and D=252 nm. (c), (d) The big sample with p=1280 nm and D=390 nm.

the microphone, thus largely reducing the effects of the scattered light. This way we can directly measure the near field absorption, and possibly catch the effects that would be otherwise hidden with other scattering dependent techniques. PA technique has been widely used for the imaging of plasmonic nanoparticles for biomedical applications, dealing with the localized surface plasmons.[19–21] Moreover, it was recently applied to study semiconductor nanowires,[22] and their resonant absorption,[23] as well as chirality when nanowires are partially covered with gold.[24,25] However, to our knowledge little work has been done on the detection of propagating surface plasmon polaritons by means of PA technique.

Our PA and optical transmission set-up is shown in Fig. 2: the samples are shined from the air side with a fixed wavelength and modulated intensity laser source, $\lambda \approx 532$ nm, having an output power of 15 mW, and being focused on the sample with a beam waist of 2.7 μm. This wavelength has been selected since it is shorter than those associated with a strong reflection by gold, so as a much higher power of the laser would be necessary, while it is still longer than the plasma wavelength

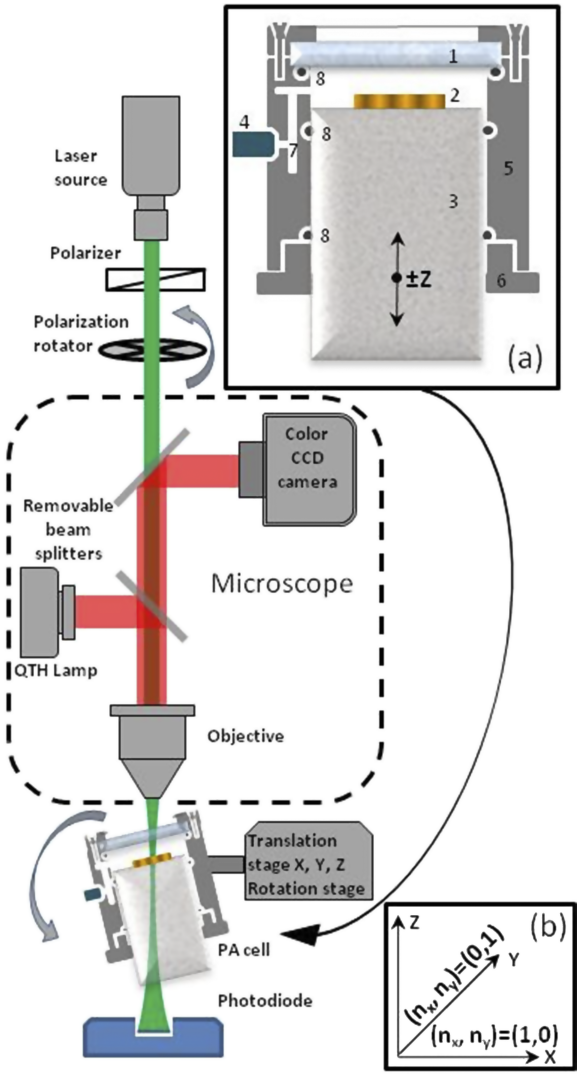

FIG. 2. Measurement set-up of the photo-acoustic and transmission techniques. Inset (a): Variable volume photoacoustic cell, 1-window(CaF_2), 2-sample, 3-quartz cylinder 50 mm DIA, 4-microphone, 5-inox cell body, 6-threaded flange, 7-sound labyrinth, 8-O-ring. Inset (b): Coordinate system where incidence angle Θ corresponds to the rotation of the x-z plane around y-axis, and the polarizations $\varphi = 0^0$ and $\varphi = 90^0$ correspond to the alignment of the electric field with the Bloch orders of the sample $(n_x, n_y) = (1, 0)$ and $(n_x, n_y) = (0, 1)$, respectively.

of gold in our samples. The output of the microphone pre-amplifier (PA), or of the photodiode (transmission measurements), is connected with the input of the lock-in amplifier and analyses the signal with respect to the modulated frequency (36 Hz) of the laser source. The schematic diagram of the variable volume closed PA cell is shown in the inset (a) of the Fig. 2. The main element of the cell is a movable transparent quartz cylinder, with two optically polished faces, which offers some advantages: its movement in z direction changes the distance between the sample surface and the window, so that we can choose the optimum volume of the cell. Moreover, in some conditions this transparent cylinder enables the comparative measurement of the PA effect and the transmission; the scattered part of the light exits from the cell to the cylinder and does not contribute to the noise increase. Our previous results[16] proved the stability and repeatability of the experiments done with this set-up.

The sample (together with the PA cell) can be rotated in the *x*-*z* plane around *y* axis, allowing for various angles of incidence θ. We have the possibility to spatially scan the samples in all three directions, with the pass of *x*-*y* scan being 500 nm, as well as we can change the input beam polarization. Our horizontal $\varphi = 0^0$ and vertical $\varphi = 90^0$ polarizations are aligned with $(n_x, n_y) = (1,0)$ and $(n_x, n_y) = (0,1)$ Bloch wave orders of the sample, respectively, as shown in the inset (b) of the Fig. 2. The measured PA signal is in all following cases normalized to the signal collected from the parts of the sample where no holes are present, under the same polarization and incidence.

In Fig. 3(a) the PA spatial scan results are shown for the *small* sample with $p = 744nm$, under the normal and different oblique angles of the input beam. The PA signal obviously follows the geometrical features (see Fig. 1(b)) accurately: under normal incidence there is already a 20% enhancement

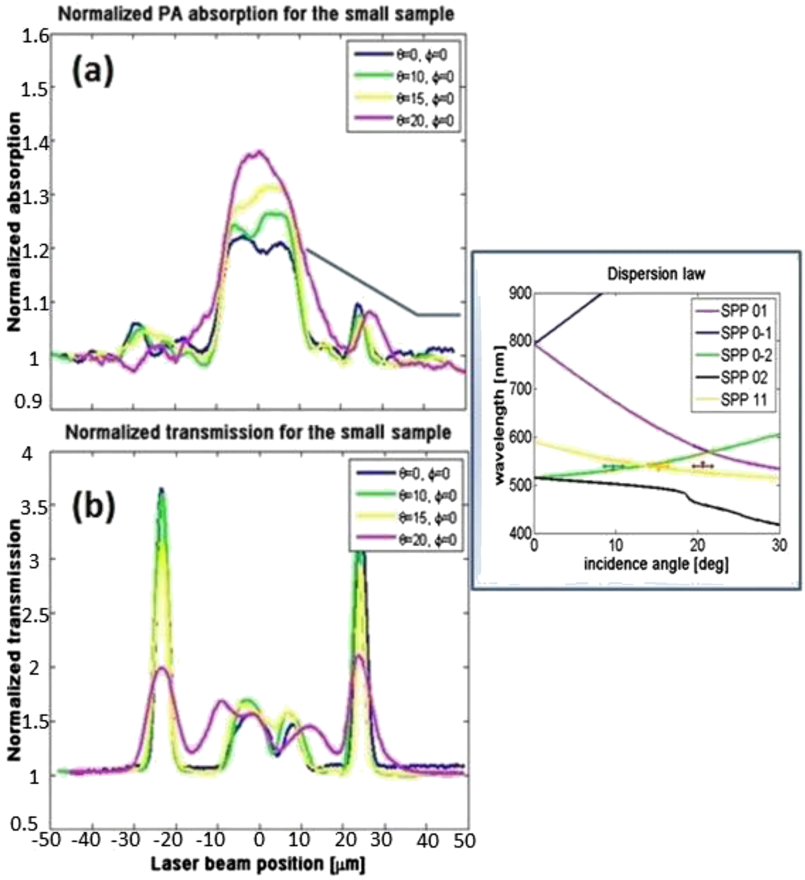

FIG. 3. (a) PA, and (b) transmission spatial scan for the *small* sample under the following light incident angles: blue - 0^0, green - 10^0, yellow - 15^0 and magenta - 20^0. Inset (a) Dispersion curves of SPP of our interest; the colored crosses correspond to the experimental points where we have measured the absorption enhancement.

in the periodic part of the array, because the light gets directly absorbed in the regions of the holes where there is Cr that absorbs more strongly with respect to Au, so the heat gets more easily spread because of the nanoholes. There is also an enhancement in the part that corresponds to the position of the scattering ring (at about 25 μm from the center of the scan). We attribute the absorption enhancement at 15° and 10° to the excitations of SPP (1,1) and SPP Au-air (0,-2), respectively. The strong resonance due to SPP (0,1) is shifted from the enhancement that we observe at 20^o, therefore we attribute this enhancement to the vicinity of both SPP (0,1) and SPP (1,1). In the inset of Fig. 3(a) we show the dispersion laws of these SPPs, underlining the experimental points where we have measured the absorption enhancement. We then compared PA results with those obtained by transmission measurements, realized by performing similar spatial scanning, Fig. 3(b): the scans reproduce the before mentioned non-resonant continuous contribution of the direct scattering through the part containing the subwavelength holes, as well as the large enhancement due to the presence of the scattering ring, but we see no apparent enhancement due to the excitation of SPP at proper angles at 532 nm.

According to Eq. (1), for the *big* sample with $p = 1280$nm under 11° incidence there are no SPP that can be excited, and we do not see any noticeable enhancement of the PA signal at 532nm (Fig. 4(a) and Fig. 4(a) inset). However, at 20° there could be a possible interplay between SPP (0,2), SPP (2,1) and SPP (1,2), and we see a 40% enhancement, confirmed by the dispersion law of these SPPs (inset of Fig. 4(a)). The corresponding transmission mapping, Fig. 4(b), again does not show a considerable angle dependence, as well as it does not show polarization dependence (not shown here). We can therefore conclude that far-field transmission data do not catch the effect of surface plasmon polaritons excited at this wavelength, while PA technique directly measures the power absorbed as the non-radiative release of energy into heat due to their traveling at the structure's surface. Moreover, at this wavelength SPP propagation length is less than micron, but PA technique still allows to monitor

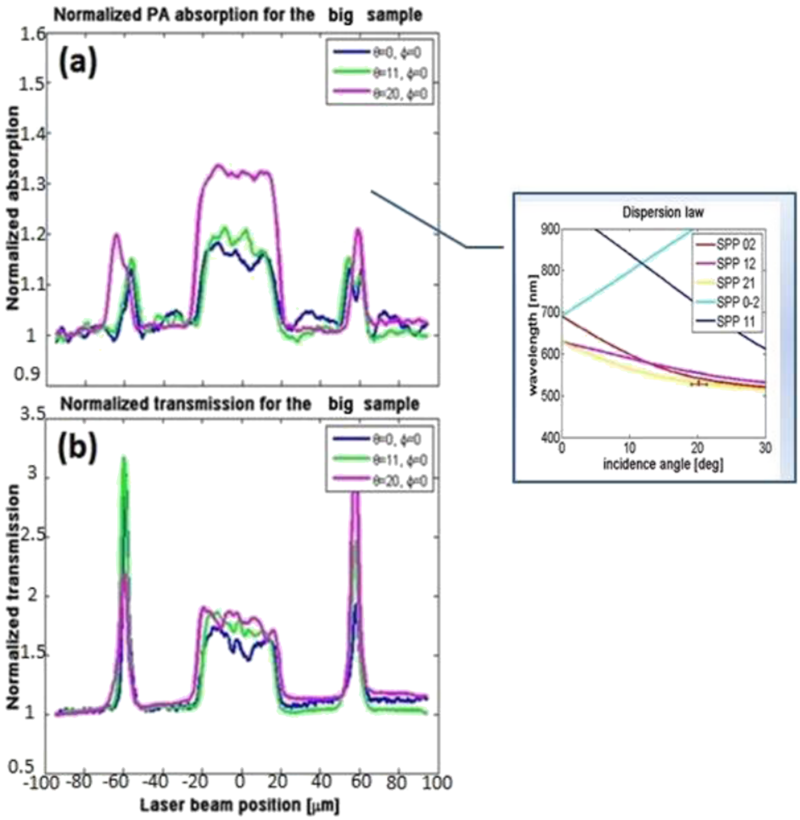

FIG. 4. (a) PA, and (b) transmission spatial scan signal for the big sample under the following incident angles: blue - 0^0, green - 11^0, and magenta - 20^0. Inset (a) Dispersion curves of SPP of our interest; the colored cross corresponds to the experimental points where we have measured the absorption enhancement.

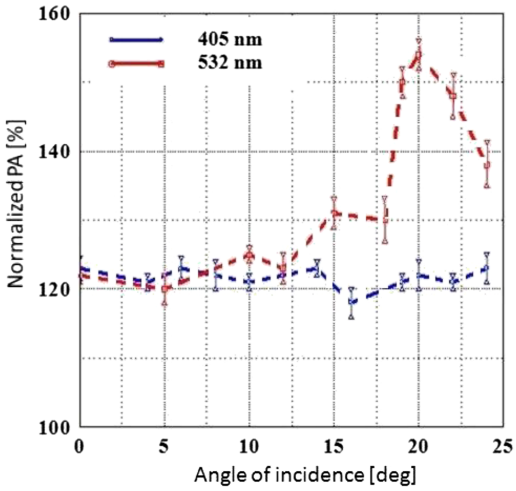

FIG. 5. PA normalized absorption dependence on the angle of incidence for the small sample, when it is shined by 405 nm and 532 nm. The average values and the errors are obtained from the analysis of the PA ±5μm from the center.

the changes in the absorption due to this decay. These features depend on the pitch since the excitation angles that lead to this behavior directly depend on the pitch (Eq. 1).

To check the validity of our results, we measured the angle dependence under a wavelength where we do not expect SPPs, namely at 405 nm. In Fig. 5 we show PA normalized to the multilayer without nanoholes for the *small* sample; the average values and the errors are obtained from the analysis of the PA ±5μm from the center. As expected, the blue curve does not show any particular maxima, while the red curve shows the maxima previously presented. We also checked the polarization dependence; under normal incidence both polarizations give the same PA signal, in agreement with the symmetry of the structure.[16]

In conclusion, we have demonstrated that PA technique can be employed as a simple and reliable plasmonic characterization technique that measures the angle dependence of the enhancement in the absorption due to the BW SPP excitation. Our results evidence a considerable absorption enhancement under proper incidence angles for 2D arrays of nanoholes with different periodicities, which is ascribed to the phase matching conditions for SPP propagation. We also show that far-field transmission measurements fail to catch these effects. Present efforts are dedicated to specific improvements of our stable and low-cost PA set-up to allow for the use of different wavelengths, better-suited for both qualitative and quantitative characterization of samples to be used for the realization of plasmonic circuits or SERS biosensing platforms.

The authors are indebted with Marco Magi for technical support.

[1] S. A. Maier, "*Plasmonics: Fundamentals and Applications*," Springer Science & Business Media (2007).
[2] M. Couture, Y. Liang, H. P. Poirier Richard, R. Faid, W. Peng, and J. F. Masson, Nanoscale **5**, 12399 (2013).
[3] S. Chang, S. Gray, and G. Schatz, Opt. Express **13**, 3150 (2005).
[4] J. A. Porto, F. J. Garcia-Vidal, and J. B. Pendry, Phys. Rev. Lett. **83**, 2845 (1999).
[5] C. Genet, M. P. van Exter, and J. P. Woerdman, Opt. Commun. **225**, 33 (2003).
[6] E. Popov, N. Bonod, M. Neviere, H. Rigenault, P.-F. Lenne, and P. Chaumet, Appl. Opt. **44**, 2332 (2005).
[7] F. J. Garcia de Abajo, Rev. Mod. Phys. **79**(4), 1267 (2007).
[8] N. Papasimakis, V. A. Fedotov, A. S. Schwanecke, N. I. Zheludev, and F. J. Garcia de Abajo, Appl. Phys. Lett. **91**, 081503 (2007).
[9] Z. Ruan and M. Qiu, Phys. Rev. Lett. **96**, 233901 (2006).
[10] L. Solomon, F. Grillot, A. V. Zayats, and F. De Fornel, Phys. Rev. Lett. **86**, 1110–1113 (2001).
[11] W. L. Barnes, A. Dereux, and T. W. Ebbesen, Nature **424**, 824 (2003).
[12] J. Xu, P. Guan, P. Kvasnička, H. Gong, J. Homola, and Q. Yu, J. Phys. Chem. C **115**, 10996 (2011).
[13] A. V. Krasavin and A. V. Zayats, Opt. Express **18**, 11791 (2010).
[14] A. Benedetti, M. Centini, C. Sibilia, and M. Bertolotti, J. Opt. Soc. Am. B **27**, 408 (2010).
[15] S. Tuccio, M. Centini, A. Benedetti, and C. Sibilia, J. Opt. Soc. Am. B **30** (2013).
[16] F. A. Bovino, V. Mussi, G. Leahu, A. Benedetti, E. Petronijevic, and C. Sibilia, in 2015 Fotonica AEIT Italian Conference on Photonics Technologies, Turin, Italy, 2015.

[17] R. Inagaki, K. Kagami, and E. T. Arakawa, Phys. Rev. B **24**, 3644R (1981).
[18] R. Inagaki, K. Kagami, and E. T. Arakawa, Appl. Opt. **21**, 949 (1982).
[19] C. W. Van Neste, L. R. Senesac, and T. Thundat, Appl. Phys. Lett. **92**, 234102 (2008).
[20] A. Feis, C. Gellini, P. R. Salvi, and M. Becucci, Photoacoustics **2**(1), 47 (2014).
[21] W. Li and X. Chen, Nanomedicine **10**(2), 299 (2015).
[22] S. I. Zelewski, J. Kopaczek, W. M. Linhart, F. Ishikawa, S. Shimomura, and R. Kudrawiec, Appl. Phys. Lett. **109**, 182106 (2016).
[23] G. Leahu, E. Petronijevic, A. Belardini, M. Centini, R. Li Voti, T. Hakkarainen, E. Koivusalo, M. Guina, and C. Sibilia, submitted to Sci. Rep. (2017).
[24] A. Belardini, M. Centini, G. Leahu, D. C. Hooper, R. Li Voti, E. Fazio, J. W. Haus, A. Sarangan, V. K. Valev, and C. Sibilia, Sci. Rep. **6**, 31796 (2016).
[25] G. Leahu, E. Petronijevic, A. Belardini, M. Centini, T. Hakkarainen, E. Koivusalo, M. R. Piton, S. Suomalainen, M.Guina, and C. Sibilia, submitted to Adv. Opt. Mat. (2017).